Published in final edited form as:
Biochemistry. 2008 June 3; 47(22): 5986–5995.

Bone sialoprotein binding to matrix metalloproteinase-2 alters enzyme inhibition kinetics†

Alka Jain‡, **Larry W. Fisher**§, and **Neal S. Fedarko**‡,*

‡ *Johns Hopkins University School of Medicine*

§ *National Institute for Dental and Craniofacial Research, National Institutes of Health*

Abstract

Bone sialoprotein (BSP) is a secreted glycophosphoprotein normally restricted in expression to skeletal tissue that is also induced by multiple neoplasms in vivo. Previous work has shown that BSP can bind to matrix metalloproteinase-2 (MMP-2). Because of MMP-2 activity in promoting tumor progression, potential therapeutic inhibitors were developed, but clinical trials have been disappointing. The effect of BSP on MMP-2 modulation by inhibitors was determined with purified components and in cell culture. Enzyme inhibition kinetics were studied using a low-molecular weight freely diffusable substrate and purified MMP-2, BSP, and natural (tissue inhibitor of matrix metalloproteinase-2) and synthetic (ilomastat and oleoyl-*N*-hydroxylamide) inhibitors. We determined parameters of enzyme kinetics by varying substrate concentrations at different fixed inhibitor concentrations added to MMP-2 alone, MMP-2 and BSP, or preformed MMP-2-BSP complexes and solving a general linear mixed inhibition rate equation with a global curve fitting program. Two in vitro angiogenesis model systems employing human umbilical vein endothelial cells (HUVECs) were used to follow BSP modulation of MMP-2 inhibition and tubule formation. The presence of BSP increased the competitive K_I values between 15- and 47-fold for natural and synthetic inhibitors. The extent of tubule formation by HUVECs cocultured with dermal fibroblasts was reduced in the presence of inhibitors, while the addition of BSP restored vessel formation. A second HUVEC culture system demonstrated that tubule formation by cells expressing BSP could be inhibited by an activity blocking antibody against MMP-2. BSP modulation of MMP-2 activity and inhibition may define its biological role in promoting tumor progression.

Keywords

Bone sialoprotein; matrix metalloproteinase; enzyme kinetics

The small integrin binding ligand N-linked glycoprotein (SIBLING)[1] gene family is clustered on human chromosome 4, and its members include bone sialoprotein (BSP), osteopontin, dentin matrix protein 1, matrix extracellular phosphoglycoprotein, and dentin sialophosphoprotein (1). BSP was once thought to be restricted in expression to mineralizing tissues such as bones and teeth (2) but has been shown to be induced in certain neoplasms

†This research was supported in part by Department of Defense grants DAMD 17-02-0684 (N.S.F.) and W81XWH-04-1-0844 (N.S.F.); NIH grant CA113865 (N.S.F.) and by the Intramural Research Program of the NIH, NIDCR (L.W.F.).

*Department of Medicine, Room 5A-64 JHAAC, 5501 Hopkins Bayview Circle, Johns Hopkins University, Baltimore, MD 21224. Phone: 410 550-2632; Fax: 410 550-1007, ndarko@jhmi.edu.

[1]The abbreviations used are: SIBLING, Small, Integrin-Binding LIgand, N-linked Glycoprotein; BSP, bone sialoprotein; MMP, matrix metalloproteinase; proMMP, pro-matrix metalloproteinase; HUVEC, human umbilical vein endothelial cell; CCK-8, (2-(2-methoxy-4-nitrophenyl)-5-(2,4-disulfophenyl-2*H*-tetrazolium monosodium salt); TIMP, tissue inhibitor of metalloproteinase; HRP, horseradish peroxidase; OA-Hy, oleoyl-N-hydroxylamide.

(3–11). SIBLINGs can be localized to the cell surface through binding of αVβ3 (as well as other integrins), and at least OPN and DMP1 can be bound by variants of CD44 (12–14), exhibit correlation between expression levels and tumor stage (15), and bind to and confer activity on specific latent matrix metalloproteinases (proMMPs) (16). Indeed, BSP has been shown to enhance the invasion potential of a number of human cancer cell lines in vitro by bridging MMP-2 to the cell surface of the cells through the αVβ3 integrin (14).

MMPs make up a family of structurally and functionally related endoproteinases that are involved in development and tissue repair as well as cancer angiogenesis and metastasis. We have recently shown that active MMPs inhibited by tissue inhibitors of metalloproteinases (TIMPs) can be reactivated by equimolar amounts of the appropriate SIBLING partner (16). The study presented here was undertaken to determine whether the mechanism of BSP action on MMP-2 activity involves the alteration of MMP affinity for TIMP2 and/or low-molecular weight inhibitors. The biological consequences of these interactions were tested using two in vitro model systems of angiogenesis.

MATERIALS AND METHODS

Reagents

ProMMP-2 and active human MMP-2 were obtained from Oncogene Research Products (Boston, MA) and Research Diagnostic Systems, Inc. (Minneapolis, MN). The inhibitors ilomastat {*N*-[(2*R*)-2-(hydroxamidocarbonylmethyl)- 4-methylpentanoyl]-L-tryptophan methylamide} and oleoyl-*N*-hydroxylamide, substrate Ac-PLG-(2-mercapto-4-methylpentanoyl)-LG-OC_2H_5, and 5,5'-dithiobis(2-nitrobenzoic acid) *(*DTNB) were obtained from Calbiochem (La Jolla, CA). Fluorescein-conjugated gelatin (fluorescein-gelatin) was obtained from Molecular Probes, Inc. (Eugene, OR). A cell counting kit containing the water-soluble tetrazolium salt CCK-8 [2-(2-methoxy-4-nitrophenyl)-5-(2,4-disulfophenyl- 2*H*-tetrazolium monosodium salt)] was purchased from Dojindo Molecular Technologies (Gaithersberg, MD). Human serum adsorbed goat anti-rabbit IgG conjugated to horseradish peroxidase (HRP) was obtained from Kirkegaard & Perry (Gaithersburg, MD). Recombinant human BSP and BSPKAE (where the RGD sequence has been changed to KAE) that included post-translational modifications were made using an adenovirus constructs and eukaryotic cells and purified (>95% purity as defined by acrylamide gel electrophoresis) as previously described (12). An activity blocking antibody against MMP-2 was obtained from Chemicon International (Temecula, CA).

Low-Molecular Weight Substrates

The activities of wildtype MMP-2 in the presence and absence of inhibitors (TIMP2, ilomastat, or oleoyl-*N*-hydroxylamide) and BSP were measured using a low-molecular weight thiopeptide substrate [Ac-PLG-(2-mercapto-4-methylpentanoyl)- LG-OC_2H_5]. Substrate was incubated in assay buffer [50 mM HEPES, 10 mM $CaCl_2$, 0.05% Brij 35, and 1 mM DTNB (pH 7.5)] with 10 nM MMP-2 and different concentrations of inhibitor, a 10 nM MMP-2-BSP preformed complex or an MMP-2-inhibitor-BSP complex added simultaneously. Data from the first 6 min were used to calculate velocity (picomoles per second) values. Substrate cleavage was monitored using a Perkin-Elmer Victor 2 multilabel plate reader, and absorbance was measured at 412 nM. Preformed MMP-2-BSP complexes were formed by incubation at 37 ° C for 30 min prior to addition to the reaction mixture. Global curve fitting of the family of substrate-velocity curves was performed using Prism 4 (GraphPad Software, Inc.) with V_{max}, K_m, K_{ic}, and K_{iu} set as shared parameters.

Coculture Angiogenesis Assay

Human umbilical vein endothelial cell (HUVEC) and human dermal fibroblast cocultures were grown in EGM-2 growth medium obtained from TCS Cell Works (Botolph Claydon, U.K.). The functional readout from this in vitro assay was tubule formation. Tubule formation was defined by the total number of tubules and number of branches. Test conditions were run in triplicate wells with eight conditions per 24-well plate. The cells were treated starting on day 6 of culture with multiple conditions, including 5 nM bFGF, 5 nM BSP, 5 nM BSPKAE, 5 nM TIMP2, 5 nM BSP and 5 nM TIMP2, 5 nM ilomastat, 5 nM ilomastat and 5 nM BSP, 33.6 nM oleoyl-*N*-hydroxylamide, 33.6 nM oleoyl-*N*-hydroxylamide and 5 nM BSP, or buffer alone. Medium was replaced every other day with fresh medium containing the positive control bFGF, BSP, BSP-KAE, and/or inhibitors. Cells were fixed in 70% ethanol on day 12, and tubule formation was quantified following immunostaining with a mouse anti-human PECAM-1 monoclonal antibody (TCS Cell Works), and secondary antibody with the substrate 5-bromo-4-chloro-3-indolyl phosphate/ nitro blue tetrazolium (BCIP/NBT, from Sigma). Images were visualized on a Nikon Diaphot inverted microscope and digitized with a Polaroid CCD digital camera and software. Two images per well were captured and digitized, and the number of tubules, the number of branch points (junctions) between tubules, and the total tubule length (in pixels) were determined using AngioSys version 1.0 (TCS Cell Works).

For MMP activity assays, a membrane-associated fraction was prepared from the HUVEC cocultures essentially as described by Ward et al. (17). Briefly, cells were scraped from culture wells in cold 5 mM Tris-HCl (pH 7.8) and homogenized, and crude membranes were prepared by centrifugation of the cell lysate at 10000*g* for 15 min at 4 °C. The supernatant was centrifuged at 105000*g* for 1 h at 4 °C; then, the supernatant was removed, and the membrane fraction was resuspended in 20 mM Tris-HCl (pH 7.8), 10 mM $CaCl_2$, and 0.05% Brij 35. A 20 μL aliquot of the membrane fraction pool was added to 12.5 μg/mL fluoresceinconjugated gelatin substrate conjugate in a 200 μL total volume of reaction buffer containing 50 mM Tris (pH 7.6), 150 mM NaCl, and 5 mM $CaCl_2$ as previously described (16). This substrate is highly substituted with fluorescein moieties so that the fluorescent signal is self-quenched until proteolytic cleavage liberates fragments and a robust fluorescent emission is measured. Fluorescence data were acquired with excitation at 485 nm and emission at 535 nm. Reactions were run in triplicate.

Collagen Sandwich Angiogenesis Assay

HUVECs were transfected with 10^4 pfu adenovirus/cell for 24 h in EGM-2 defined medium. The adenovirus contained the coding sequence for normal BSP (12) or was the null (empty) Ad5 virus. Cells were then released from the flasks by trypsin/ EDTA treatment, counted with a hemocytometer, and then seeded at a density of 10^4 cells/well onto wells that had been coated with type I collagen and allowed to gel. The collagen sandwich was made by mixing 8 volumes of a cold type acid-soluble 3 mg/mL type I collagen solution (pH 3.0) (Cellmatrix, Nitta, Osaka, Japan) with 1 volume of cold 10x concentrated MEM buffer without NaHCO3. The solution was carefully mixed, while on ice, an additional 1 volume of reconstitution buffer (2.2 g of $NaHCO_3$ in 100 mL of 0.05 N NaOH and 200 mM HEPES) was added and mixed. Wells of a 48-well plate were coated with 150 μL of the solution, and the plate was placed in a 37 °C incubator with 5% CO2 for 30 min to gel the solution. Cells were added to each well in a volume of 150 μL, and the plate was returned to the tissue culture incubator to enable cell attachment. After 2 h at 37 °C, the unattached cells in solution were aspirated from the wells, the wells were rinsed twice with serum-free medium, and a second 150 μL portion of the collagen solution was added to each well. After 30 min at 37 °C, endothelial cell basal medium (EBM-2, Cambrex Corp.) with or without 1.25 μg of an activity blocking anti-MMP-2 antibody was added to each well and HUVECs were grown in culture for up to an additional 48 h.

The cell number in the collagen gel culture system was followed by using the addition of CCK-8 to the medium at the start of the experiments following the manufacturer's protocol. CCK-8, which is less toxic then other tetrazolium salts such as MTT and can be used to monitor cell proliferation over days of continuous culture, is metabolized by cells to form a formazan dye whose absorbance value at 460 nm is directly proportional to the number of living cells. The fluorescein-conjugated gelatin substrate was used to follow MMP proteolytic activity in the collagen gels. A solution of 12.5 μg/mL fluorescein-substrate conjugate was added to the bottom collagen gel prior to polymerization. Fluorescence data were acquired with excitation at 485 nm and emission at 535 nm using a Victor 2 Multilabel plate analyzer. MMP enzyme activity was measured as the rate of change in fluorescence per minute, with the slope over the first 10 min determined. Zymography for MMP detection and Western blotting for profiling BSP protein expression were performed exactly as previously described (16).

RESULTS

TIMP Inhibition Kinetics

To determine the effect of BSP on active wild-type MMP-2 and TIMP2 reaction kinetics, a low-molecular weight substrate was employed to follow product evolution over time. MMP-2 incubated with increasing concentrations of TIMP2 exhibited the expected dose-dependent inhibition (Figure 1A). The level of inhibition by TIMP2 was significantly decreased either by the presence of a preformed MMP-2-BSP complex or by the simultaneous addition of BSP and TIMP2 to MMP-2 (Figure 1B,C). To investigate whether a decreased level of inhibition of MMP-2 by TIMP2 in the presence of BSP was associated with an altered affinity, we obtained substrate-velocity plots by varying substrate concentrations of each at different but fixed inhibitor concentrations. Reaction conditions included either TIMP2 and 10 nM MMP-2, TIMP2 and 10 nM preformed equimolar MMP-2-BSP complexes, or simultaneous mixes of TIMP2, 10 nM MMP-2, and 10 nM BSP (Figure 1D–F).

Because there are two distinct binding sites for TIMP2 on MMP-2, TIMP2 does not act purely as a competitive inhibitor (18). The common types of inhibition (competitive, uncompetitive, and noncompetitive) are all special cases of linear mixed inhibition (19). The generalized linear mixed inhibition equation $V = V_{max}[S]/[K_m(1 + [I]/K_{ic}) + [S](1 + [I]/K_{iu})]$ was employed to determine the reaction rate, where V_{max} is the limiting rate, K_m is the Michaelis constant, K_{ic} is the competitive inhibition constant, and K_{iu} is the uncompetitive inhibition constant. For competitive inhibition, $[I]/K_{iu}$ is negligible, while for uncompetitive inhibition, $[I]/K_{ic}$ is negligible. In pure noncompetitive inhibition, the inhibition constants are equal.

Global curve fitting of the family of substrate-velocity curves revealed a significant increase in K_{ic} and K_{iu} values for the MMP-2-BSP complex as well as the simultaneously added MMP-2 and BSP (Table 1). The inhibitor TIMP2 had K_{ic} and K_{iu} values for the MMP-2-BSP preformed complex increased 36- and 6-fold, respectively. The K_{ic} and K_{iu} values were increased 15- and 6-fold, respectively when all components were added simultaneously. These values indicate a relatively poor affinity of the inhibitor for MMP-2 in the presence of BSP. The fitted values for K_m and V_{max} were not significantly different with or without TIMP2 or BSP. The order of magnitude change in the apparent inhibitor affinity for MMP-2 in the presence of BSP indicates that SIBLING modulation of MMPs may be physiologically significant.

Low-Molecular Weight Inhibitor Kinetics

The MMP inhibitors ilomastat and oleoyl-*N*-hydroxylamide were utilized to test whether low-molecular weight drug inhibition of MMP-2 activity could be modulated by BSP. Ilomastat at a concentration of 1 nM inhibited the initial velocity of MMP-2 activity to 39% of control activity, while the same concentration of inhibitor reduced the activity of the MMP-2 with BSP

to only 70% of the control, suggesting that the inhibitor is much less effective against MMP-2 in the conformation resulting from the binding of BSP (Figure 2A). Similar to the studies with TIMP2, substrate-velocity plots of the enzyme activity of MMP-2 in the presence of different concentrations of ilomastat reacted with increasing substrate concentrations in the presence or absence of BSP were made. BSP reduced the level of inhibition by ilomastat whether it was added as a preformed complex with MMP-2 (Figure 2C) or added simultaneously to MMP-2 with the inhibitor (Figure 2D). Because ilomastat is a competitive inhibitor, kinetic parameters in the presence and absence of BSP can be determined by fitting the substrate-velocity curves to the equation for competitive inhibition $v = V_{max}[S]/K_m(1 + [I]/K_{ic}) + [S]$, where V_{max} is the limiting rate, K_m is the Michaelis constant, K_{ic} is the competitive inhibition constant, [S] is the substrate concentration, and [I] is the ilomastat concentration. The results indicated a significant increase (>30-fold) in the K_{ic} value of ilomastat for MMP-2 when BSP was included in the reaction mixture (Table 1). Thus, ilomastat exhibited a reduced affinity for MMP-2 in the presence of BSP.

The same substrate and reaction conditions were utilized to follow MMP-2 reaction velocities in the presence of the low-molecular weight inhibitor oleoyl-*N*-hydroxylamide. The addition of 10 μM oleoyl-*N*-hydroxylamide inhibited the activity of MMP-2 by 80%, while the inclusion of 10 nM BSP restored activity by ~50% (Figure 3A). Titration with increasing amounts of BSP revealed a dose response to the increase in enzymatic activity, with the highest dose, 100 nM BSP, restoring the activity of the inhibited enzyme to 75%. Substrate-velocity plots were made for reaction conditions of MMP-2 incubated with oleoyl-*N*-hydroxylamide alone, an MMP-2-BSP preformed complex incubated with oleoyl-*N*-hydroxylamide, and simultaneously added MMP-2, BSP, and oleoyl-*N*-hydroxylamide (Figure 3B–D). Global curve fitting of the family of substrate-velocity curves revealed a significant increase the value of K_{ic} for oleoyl-*N*-hydroxylamide in the presence of BSP (Table 1). The inhibitor oleoyl-*N*-hydroxylamide had its K_{ic} value for the MMP-2-BSP preformed complex increased 25-fold, while the K_{ic} value was increased 18-fold when all components were added simultaneously.

BSP Restores Activity to Inhibited MMPs in Vitro

The ability of BSP to restore enzymatic activity to MMP-2 inhibited by TIMP2, ilomastat, or oleoyl-*N*-hydroxylamide in a purified component assay led to a screen of the effects of BSP on MMP inhibitors in an in vitro model system with a biological readout (tubule formation). The model system used human umbilical vein endothelial cells (HUVECs) cocultured with normal adult human diploid dermal fibroblasts grown in a defined endothelial cell basal medium supplemented with EGM-2. Over the course of almost 2 weeks of culture, the endothelial cells form threadlike tubule structures and expressed endothelial cell-specific components that can be stained immunohostochemically with antibodies against PECAM-1 (Figure 4). BSP (5 nM) alone stimulated tubule formation by HUVECs above that of control. Treatment of the coculture system with a variant of BSP whose RGD sequence had been mutated to KAE (BSPKAE, which can not bind the $\alpha_v\beta_3$ integrin and is unable to be localized to the cell surface) caused a reduction in the level of tubule formation. Incubation separately with 5 nM TIMP2, 5 nM ilomastat, or 33.6 nM oleoyl-*N*-hydroxylamide inhibited tubule formation below control levels. The inclusion of BSP with MMP-specific inhibitors increased immunostained tubule structures.

Quantification of tubule formation using AngioSys version 1.0 revealed that incubation of the cells with 5 nM bFGF or 5 nM BSP alone resulted in a similar increase in tubule and junction/branching numbers (289 ± 55 tubules and 110 ± 21 branches for bFGF vs 335 ± 18 tubules and 145 ± 13 branches for BSP). Treatment with BSPKAE inhibited tubule formation by 50% and branching by 70%, relative to control (Figure 5A,B). The MMP inhibitors decreased the level of tubule formation and branching between 25 and 90%. The addition of BSP to TIMP2-,

ilomastat-, or oleoyl-*N*-hydroxylamide- treated cells significantly increased the number of tubules approximately 3-fold and the number of branch points approximately 5-fold compared to levels with inhibitor alone. The restoration of tubule formation by the addition of BSP to oleoyl-*N*-hydroxylamide-treated cells, although significant compared to conditions with inhibitor alone, was much weaker than that for control and other BSP treatment conditions. The effect of BSP on MMP activity in the in vitro coculture angiogenesis system was also studied using a large macromolecular substrate, fluorescein-gelatin, to measure MMP enzyme activity of plasma membrane preparations. When the gelatinase activity of membrane-associated MMPs was assayed in cohort wells treated under the same conditions, the pattern paralleled that of the number of tubules and branches (Figure 5C). Incubation of the cells with 5 nM bFGF alone resulted in an average membraneassociated enzyme activity of 225 ± 11 fluorescein-gelatin/ min, while 5 nM BSP was associated with 445 ± 67 fluorescein-gelatin/ min. The BSPKAE variant had a membrane-associated gelatinase activity of 78 ± 19 fluoresceingelatin/ min. MMP activity as a percentage of control values was 40% with TIMP2, 50% with ilomastat, and 10% with oleoyl-*N*-hydroxylamide. The addition of BSP to the culture medium significantly restored enzyme activity in the presence of each inhibitor ($p \leq 0.01$).

The coculture system requires multiple days of cell growth prior to tubule formation and as such was not ideal for demonstrating a direct linkage among BSP, MMP-2, and tubule formation. A second model system of angiogenesis was employed that required a much shorter time frame (14–24 h) and could be easily manipulated to incorporate MMP-specific blocking antibodies. HUVECs grown in EBM-2 medium were transfected with adenovirus for BSP, or null Ad5 virus as a negative control, and then transferred into collagen sandwiches. At 14, 24, and 48 h, cells in the collagen sandwich were visualized using a Nikon Daiphot microscope. Collagen gels containing null virus-transfected cells exhibited an isolated spherical pattern at 14 and 24 h, and by 48 h, few cells had elongated and associated to form tubules (Figure 6). In contrast, wells containing BSPtransfected cells showed cell elongation, association, and tubule formation by 14 h. The inclusion of a monoclonal antibody that specifically blocks the activity of MMP-2 with cells transfected with the BSP adenovirus in the collagen sandwich system visibly reduced the level of cell elongation and association at all time points.

Tubule formation was again quantified as the number of tubules and branches using AngioSys version 1.0. The small number of tubules in the null-transfected cells increased over the time course; however, the numbers remained relatively small (Figure 7). In the BSP adenovirus-transfected cells, the number of tubules increased between 6- and 14-fold over the 14, 24, and 48 h time points when compared to those of the null virus-transfected cells. The addition of the anti- MMP-2 antibody reduced the number of tubules 74–84%. Similarly, the number of branches remained low of the three time points in the null transfected cell, increased between 6- and 8-fold in the BSP adenovirus-transfected cells, and decreased 62–83% by the inclusion of the MMP-2 antibody. Because it is possible that the expression of BSP changed the proliferation of the cells which in turn altered tubule formation and branching, the number of cells in each well was profiled using the CCK-8 tetrazolium salt. The relative absorbance did increase to a small degree across the time points. The largest increase was observed in the BSP adenovirus cells which had a 13% increase in absorbance, while the inclusion of the MMP-2 antibody with the BSP adenovirus-transfected cells exhibited a 4% increase between 14 and 48 h. There were, however, no significant differences in cell number between any of the conditions and time points; thus, it is unlikely that effects of BSP on cell proliferation account for an increased level of tubule formation. We have observed that cells grown for more than 72 h in the collagen gel system do show differences in cell survival and cell number (data not shown). However, in the current assay, significant tubule formation occurred well before any changes in cell number.

The activity of MMPs in the gel culture system was monitored using the fluorescein-gelatin substrate. Cells transfected with the BSP adenovirus had between 3- and 5-fold higher enzyme activity then cells transfected with null virus, while the inclusion of the monoclonal antibody against MMP-2 reduced enzyme activity between 54 and 71% across the different time points. In the collagen gel system, membrane-associated MMP-2 activity was necessary for BSP-dependent tubule formation. The endothelial cells were used to test whether attachment of BSP to the cell membrane was required for tubule formation. HUVECs were transfected with null Ad5 virus, BSP, or BSPKAE adenovirus and grown in collagen gels for 24 h, and tubule formation was monitored by microscopy (Figure 8). Expression of BSP with an intact RGD sequence led to abundant tubule formation, while transfection with BSPKAE reduced the level of tubule formation below control levels. HUVECs transfected with null Ad5 virus or the BSPKAE virus had no detectable BSP in a membrane-associated pool (Figure 8D). The levels of active MMP-2 in the membrane-associated pool were elevated in the BSP-transfected cells and reduced in the BSPKAE-transfected cells. These observations are consistent BSP-dependent tubule formation requiring BSP and MMP-2 localization to the cell surface.

DISCUSSION

BSP is a member of the SIBLING gene family (2). It is extended and flexible in solution, and such a lack of ordered structure is shared by a number proteins that have multiple binding partners (1). BSP can bind the $\alpha_V\beta_3$ integrin via its RGD sequence (20,21) and to complement Factor H (12). BSP can also bind to and modulate the activity of MMP-2 (16). Binding of BSP to MMP-2 was associated with conformational changes as indicated by fluorescence quenching during BSP binding titration (indicating a change in the microenvironment of the MMP's tryptophans), and by increased susceptibility of a BSP-proMMP-2 complex to plasmin cleavage. BSP binding to pro-MMP-2 was associated with increased proteolytic activity, and BSP binding to TIMP2-inhibited MMP-2 restored activity (16). Taken together, the data suggest that conformational changes in MMP-2 induced by BSP binding may include changes in the shape of the active site and inhibitor binding domains. A trimolecular complex of BSP, $\alpha_V\beta_3$, and MMP-2 can be demonstrated by immunoprecipitation, flow cytometry, and in situ hybridization in cancer cells grown in vitro (14). BSP message was induced in multiple cancers and its expression correlated with paired MMP-2 expression as well as tumor stage (15).

MMP-2, a gelatinase that can degrade components of the extracellular matrix at physiological pH, is regulated in vivo by the naturally occurring TIMPs and RECK (22,23). TIMP2 binding to MMP-2 involves distinct domains on both the inhibitor and the enzyme (24–26). The binding and kinetics of MMP-2 and TIMP2 are more complex than simple competitive inhibition. In our analyses, we have used a mixed linear model of mixed inhibition (19) and observed inhibition constants at or below the nanomolar range. K_i values in the subnanomolar range for TIMP2 and MMP-2 using the same substrate have been reported in the literature (27–29), though a more recent analysis has yielded 3-4-fold higher estimates (30). The different reported values are most likely due to differences in sources and concentrations of substrate, enzyme, and inhibitor.

BSP was found to significantly reduce the affinity of low-molecular weight synthetic inhibitors (ilomastat and oleoyl- *N*-hydroxylamide) for MMP-2. Ilomastat as a hydroxamate class inhibitor blocks the activity of multiple MMPs and has been used to disrupt angiogenesis and metastasis (31–33). Ilomastat blocked TNFα processing (34), experimental autoimmune encephalitis (35), angiogenesis, and metastasis (31–33). The magnitude of the change in the apparent affinity of the inhibitor for MMP-2 in the presence of BSP indicates that SIBLING modulation of MMP inhibition by lowmolecular weight drugs can be physiologically significant.

Finally, cell culture model systems were used to test whether BSP modulation of MMP-2 occurs in vitro. The first model system utilized human umbilical vein endothelial cells (HUVECs) cocultured with normal adult human diploid dermal fibroblasts. The endothelial cells form small islands among the fibroblasts, proliferate, and migrate through the coculture matrix to form threadlike tubule structures. These cordlike structures join up to form a network of anastomosing tubules (36). The observed effects of BSP (stimulating basal tubule formation and restoring formation to TIMP2-, ilomastat-, or oleoyl-*N*-hydroxylamide-inhibited cultures) were consistent with BSP modulating MMP-2 activity. BSPKAE, which lacks the ability to bind to cell surface receptors, did not stimulate tubule formation. Profiling MMP-2 activity in the in vitro coculture system (by fluorescent substrate assays) demonstrated changes with BSP or BSPKAE treatment consistent with a requirement for BSP cell surface localization for BSP-dependent activity. The HUVEC culture in the collagen gel system similarly exhibited an increased level of tubule formation when cells expressed BSP. The inclusion of an activity-blocking antibody to MMP-2 significantly reduced the level of BSP-dependent tubule formation. Transfection with BSPKAE also led to a decreased level of tubule formation which was associated with reduced levels of active MMP-2 at the cell surface. In both culture systems, MMP enzyme activity correlated with the extent of tubule formation and presence of BSP. Thus, BSP promotion of HUVEC tubule formation most likely acts through BSP cell surface localization and the modulation of MMP-2 activity. It has been reported that BSP promotes angiogenesis in the chick chorioallantoic membrane system (37). These results indicate that BSP has biochemical and biological plausibility to be playing active roles in tumor progression in vivo. BSP is induced by multiple neoplasms in vivo, and its modulation of inhibitor affinity for MMP-2 might contribute to the relative lack of efficacy seen in the recent clinical trials of MMP inhibitors in numerous cancers (38). This suggests that the screening of new inhibitors of MMPs for potential therapeutic use should be done in the presence of BSP.

Acknowledgements

TIMP2 was a generous gift of Dr. H. Birkedal-Hansen (National Institute of Dental and Craniofacial Research, National Institutes of Health).

References

1. Fisher LW, Torchia DA, Fohr B, Young MF, Fedarko NS. The solution structures of two SIBLING proteins, bone sialoprotein and osteopontin, by NMR. Biochem Biophys Res Commun 2001;280:460–465. [PubMed: 11162539]
2. Fisher LW, Fedarko NS. Six genes expressed in bones and teeth encode the current members of the SIBLING family of proteins. Connect Tissue Res 2003;44:33–40. [PubMed: 12952171]
3. Bellahcene A, Menard S, Bufalino R, Moreau L, Castronovo V. Expression of bone sialoprotein in primary human breast cancer is associated with poor survival. Int J Cancer 1996;69:350–353. [PubMed: 8797881]
4. Ibrahim T, Leong I, Sanchez-Sweatman O, Khokha R, Sodek J, Tenenbaum HC, Ganss B, Cheifetz S. Expression of bone sialoprotein and osteopontin in breast cancer bone metastases. Clin Exp Metastasis 2000;18:253–260. [PubMed: 11315099]
5. Fedarko NS, Jain A, Karadag A, Van Eman MR, Fisher LW. Elevated serum bone sialoprotein and osteopontin in colon, breast, prostate, and lung cancer. Clin Cancer Res 2001;7:4060– 4066. [PubMed: 11751502]
6. Woitge HW, Pecherstorfer M, Horn E, Keck AV, Diel IJ, Bayer P, Ludwig H, Ziegler R, Seibel MJ. Serum bone sialoprotein as a marker of tumour burden and neoplastic bone involvement and as a prognostic factor in multiple myeloma. Br J Cancer 2001;84:344–351. [PubMed: 11161399]
7. Carlinfante G, Vassilioul D, Svensson O, Wendel M, Heinegard D, Andersson G. Differential expression of osteopontin and bone sialoprotein in bone metastasis of breast and prostate carcinoma. Clin Exp Metastasis 2003;20:437–444. [PubMed: 14524533]

8. Detry C, Waltregny D, Quatresooz P, Chaplet M, Kedzia W, Castronovo V, Delvenne P, Bellahcene A. Detection of bone sialoprotein in human (pre)neoplastic lesions of the uterine cervix. Calcif Tissue Int 2003;73:9–14. [PubMed: 14506948]
9. Fisher LW, Jain A, Tayback M, Fedarko NS. Small integrin binding ligand N-linked glycoprotein gene family expression in different cancers. Clin Cancer Res 2004;10:8501–8511. [PubMed: 15623631]
10. Papotti M, Kalebic T, Volante M, Chiusa L, Bacillo E, Cappia S, Lausi P, Novello S, Borasio P, Scagliotti GV. Bone sialoprotein is predictive of bone metastases in resectable non-small-cell lung cancer: A retrospective case-control study. J Clin Oncol 2006;24:4818–4824. [PubMed: 17050866]
11. Ogbureke KU, Nikitakis NG, Warburton G, Ord RA, Sauk JJ, Waller JL, Fisher LW. Up-regulation of SIBLING proteins and correlation with cognate MMP expression in oral cancer. Oral Oncol 2007;43:920–932. [PubMed: 17306612]
12. Fedarko NS, Fohr B, Gehron Robey P, Young MF, Fisher LW. Factor H binding to bone sialoprotein and osteopontin enables molecular cloaking of tumor cells from complement-mediated attack. J Biol Chem 2000;275:16666–16672. [PubMed: 10747989]
13. Jain A, Karadag A, Fohr B, Fisher LW, Fedarko NS. Three SIBLINGs (small integrin-binding ligand, N-linked glycoproteins) enhance factor H's cofactor activity enabling MCPlike cellular evasion of complement-mediated attack. J Biol Chem 2002;277:13700–13708. [PubMed: 11825898]
14. Karadag A, Ogbureke KU, Fedarko NS, Fisher LW. Bone sialoprotein, matrix metalloproteinase 2, and Rv 3 integrin in osteotropic cancer cell invasion. J Natl Cancer Inst 2004;96:956–965. [PubMed: 15199115]
15. Fisher LW, Jain A, Tayback M, Fedarko NS. Small Integrin Binding LIgand N-linked Glycoprotein (SIBLING) gene family expression in different cancers. Clin Cancer Res 2004;10:8501–8511. [PubMed: 15623631]
16. Fedarko NS, Jain A, Karadag A, Fisher LW. Three small integrin binding ligand N-linked glycoproteins (SIBLINGs) bind and activate specific matrix metalloproteinases. FASEB J 2004;18:734–736. [PubMed: 14766790]
17. Ward RV, Atkinson SJ, Slocombe PM, Docherty AJP, Reynolds JJ, Murphy G. Tissue inhibitor of metalloprotienases-2 inhibits the activation of 72 kDa progelatinase by fibroblast membranes. Biochim Biophys Acta 1991;1079:242–246. [PubMed: 1911847]
18. Kleiner DE Jr, Unsworth EJ, Krutzsch HC, Stetler- Stevenson WG. Higher-order complex formation between the 72-kilodalton type IV collagenase and tissue inhibitor of metalloproteinases-2. Biochemistry 1992;31:1665–1672. [PubMed: 1310615]
19. Cortes A, Cascante M, Cardenas ML, Cornish-Bowden A. Relationships between inhibition constants, inhibitor concentrations for 50% inhibition and types of inhibition: New ways of analysing data. Biochem J 2001;357:263–268. [PubMed: 11415458]
20. Oldberg A, Franzen A, Heinegard D. Cloning and sequence analysis of rat bone sialoprotein (osteopontin) cDNA reveals an Arg-Gly-Asp cell-binding sequence. Proc Natl Acad Sci USA 1986;83:8819–8823. [PubMed: 3024151]
21. Fisher LW, McBride OW, Termine JD, Young MF. Human bone sialoprotein. Deduced protein sequence and chromosomal localization. J Biol Chem 1990;265:2347–2351. [PubMed: 2404984]
22. Giannelli G, Antonaci S. Gelatinases and their inhibitors in tumor metastasis: From biological research to medical applications. Histol Histopathol 2002;17:339–345. [PubMed: 11813883]
23. Oh J, Takahashi R, Kondo S, Mizoguchi A, Adachi E, Sasahara RM, Nishimura S, Imamura Y, Kitayama H, Alexander DB, Ide C, Horan TP, Arakawa T, Yoshida H, Nishikawa S, Itoh Y, Seiki M, Itohara S, Takahashi C, Noda M. The membrane-anchored MMP inhibitor RECK is a key regulator of extracellular matrix integrity and angiogenesis. Cell 2001;107:789–800. [PubMed: 11747814]
24. Willenbrock F, Crabbe T, Slocombe PM, Sutton CW, Docherty AJ, Cockett MI, O'Shea M, Brocklehurst K, Phillips IR, Murphy G. The activity of the tissue inhibitors of metalloproteinases is regulated by C-terminal domain interactions: A kinetic analysis of the inhibition of gelatinase A. Biochemistry 1993;32:4330–4337. [PubMed: 8476862]
25. Nguyen Q, Willenbrock F, Cockett MI, O'Shea M, Docherty AJ, Murphy G. Different domain interactions are involved in the binding of tissue inhibitors of metalloproteinases to stromelysin-1 and gelatinase A. Biochemistry 1994;33:2089–2095. [PubMed: 8117665]

26. Hutton M, Willenbrock F, Brocklehurst K, Murphy G. Kinetic analysis of the mechanism of interaction of fulllength TIMP-2 and gelatinase A: Evidence for the existence of a low-affinity intermediate. Biochemistry 1998;37:10094–10098. [PubMed: 9665714]
27. O'Shea M, Willenbrock F, Williamson RA, Cockett MI, Freedman RB, Reynolds JJ, Docherty AJ, Murphy G. Site-directed mutations that alter the inhibitory activity of the tissue inhibitor of metalloproteinases-1: Importance of the N-terminal region between cysteine 3 and cysteine 13. Biochemistry 1992;31:10146–10152. [PubMed: 1420137]
28. Murphy G, Docherty AJ. The matrix metalloproteinases and their inhibitors. Am J Respir Cell Mol Biol 1992;7:120– 125. [PubMed: 1497900]
29. O'Connell JP, Willenbrock F, Docherty AJ, Eaton D, Murphy G. Analysis of the role of the COOH-terminal domain in the activation, proteolytic activity, and tissue inhibitor of metalloproteinase interactions of gelatinase B. J Biol Chem 1994;269:14967–14973. [PubMed: 8195131]
30. Olson MW, Gervasi DC, Mobashery S, Fridman R. Kinetic analysis of the binding of human matrix metalloproteinase- 2 and -9 to tissue inhibitor of metalloproteinase (TIMP)-1 and TIMP-2. J Biol Chem 1997;272:29975–29983. [PubMed: 9368077]
31. Boghaert ER, Chan SK, Zimmer C, Grobelny D, Galardy RE, Vanaman TC, Zimmer SG. Inhibition of collagenolytic activity relates to quantitative reduction of invasion in vitro in a c-Ha-ras transfected glial cell line. J Neurooncol 1994;21:141–150. [PubMed: 7861190]
32. Galardy RE, Grobelny D, Foellmer HG, Fernandez LA. Inhibition of angiogenesis by the matrix metalloprotease inhibitor N-[2R-2- (hydroxamidocarbonymethyl)-4-methylpentanoyl)]-L-tryptophan methylamide. Cancer Res 1994;54:4715–4718. [PubMed: 7520359]
33. Winding B, NicAmhlaoibh R, Misander H, Hoegh-Andersen P, Andersen TL, Holst-Hansen C, Heegaard AM, Foged NT, Brunner N, Delaisse JM. Synthetic matrix metalloproteinase inhibitors inhibit growth of established breast cancer osteolytic lesions and prolong survival in mice. Clin Cancer Res 2002;8:1932–1939. [PubMed: 12060638]
34. Solorzano CC, Ksontini R, Pruitt JH, Auffenberg T, Tannahill C, Galardy RE, Schultz GP, MacKay SL, Copeland EM III, Moldawer LL. A matrix metalloproteinase inhibitor prevents processing of tumor necrosis factor α (TNF α) and abrogates endotoxin-induced lethality. Shock 1997;7:427–431. [PubMed: 9185243]
35. Gijbels K, Galardy RE, Steinman L. Reversal of experimental autoimmune encephalomyelitis with a hydroxamate inhibitor of matrix metalloproteases. J Clin InVest 1994;94:2177–2182. [PubMed: 7989572]
36. Bishop ET, Bell GT, Bloor S, Broom IJ, Hendry NF, Wheatley DN. An in vitro model of angiogenesis: Basic features. Angiogenesis 1999;3:335–344. [PubMed: 14517413]
37. Bellahcene A, Bonjean K, Fohr B, Fedarko NS, Robey FA, Young MF, Fisher LW, Castronovo V. Bone sialoprotein mediates human endothelial cell attachment and migration and promotes angiogenesis. Circ Res 2000;86:885–891. [PubMed: 10785511]
38. Mandal M, Mandal A, Das S, Chakraborti T, Sajal C. Clinical implications of matrix metalloproteinases. Mol Cell Biochem 2003;252:305–329. [PubMed: 14577606]

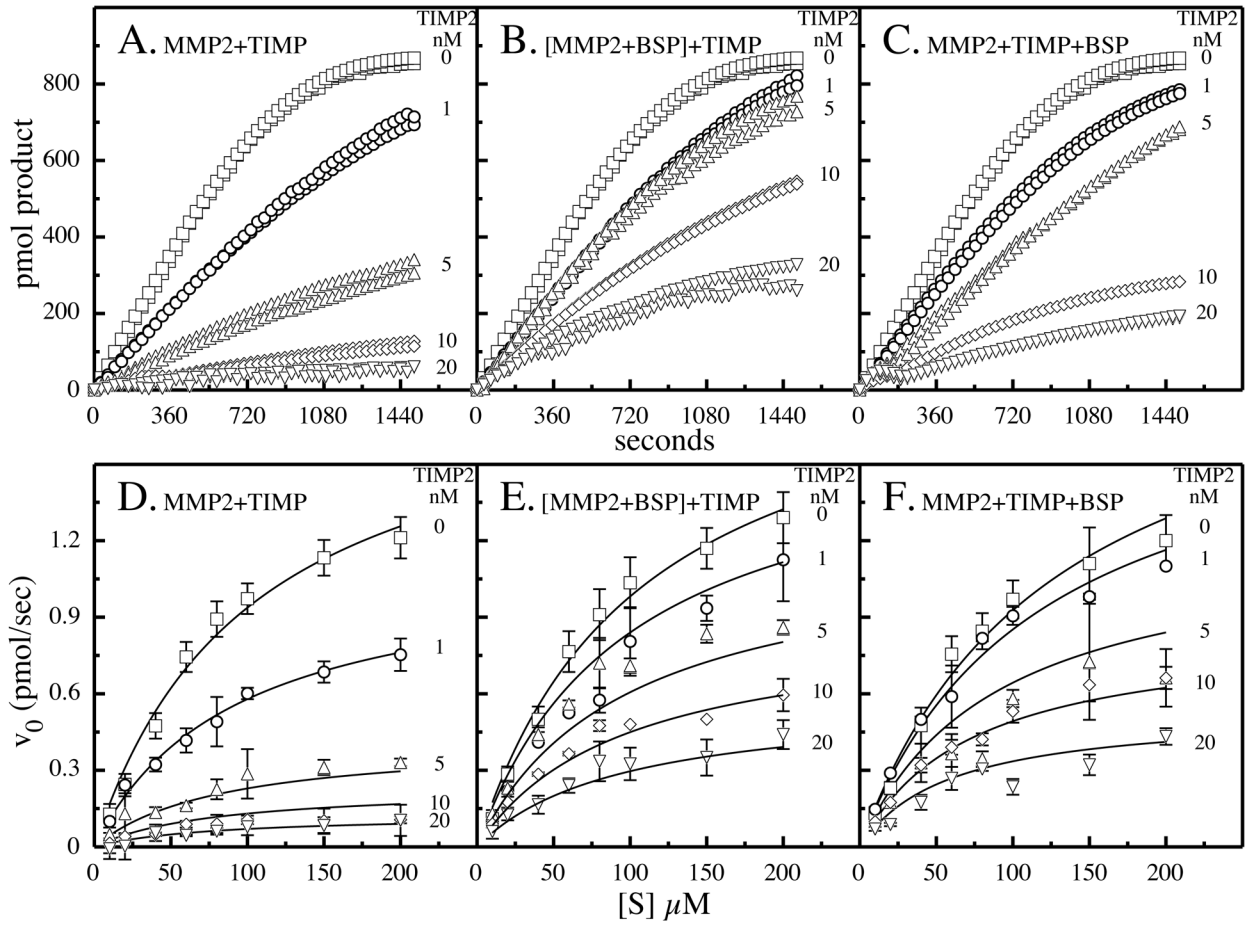

FIGURE 1.

Effects of BSP on TIMP2 inhibition of MMP-2. The substrate Ac-PLG-(2-mercapto-4-methylpentanoyl)-LG-OC_2H_5 was incubated in assay buffer at a final concentration of 100 μM with (A) 10 nM MMP-2 and different concentrations of TIMP2, (B) 10 nM MMP- 2-BSP preformed complex incubated with increasing concentrations of TIMP2, or (C) simultaneously added 10 nM MMP-2 and BSP and different concentrations of TIMP2. TIMP2 concentrations were 0 (□), 1 (○), 5 (△), 10 (◇), and 20 (▽). The concentrations MMP-2 and BSP were 10 nM. Reaction rates were profiled by increasing the substrate concentration from 10 to 200 μM. Data from the first 6 min of each reaction condition were used to calculate V_0 (picomoles per second) values. Substrate-velocity plots of MMP-2 incubated with different concentrations of TIMP2 (D), of MMP-2-BSP complexes incubated with varying concentrations of TIMP2 (E), or of MMP-2 incubated simultaneously with TIMP2 and BSP (F) were determined. MMP-2-BSP preformed complexes were formed by incubation at 37 °C for 30 min prior to addition to the reaction mixture. Six separate experiments were combined for each condition, and values represent the mean ± the standard deviation.

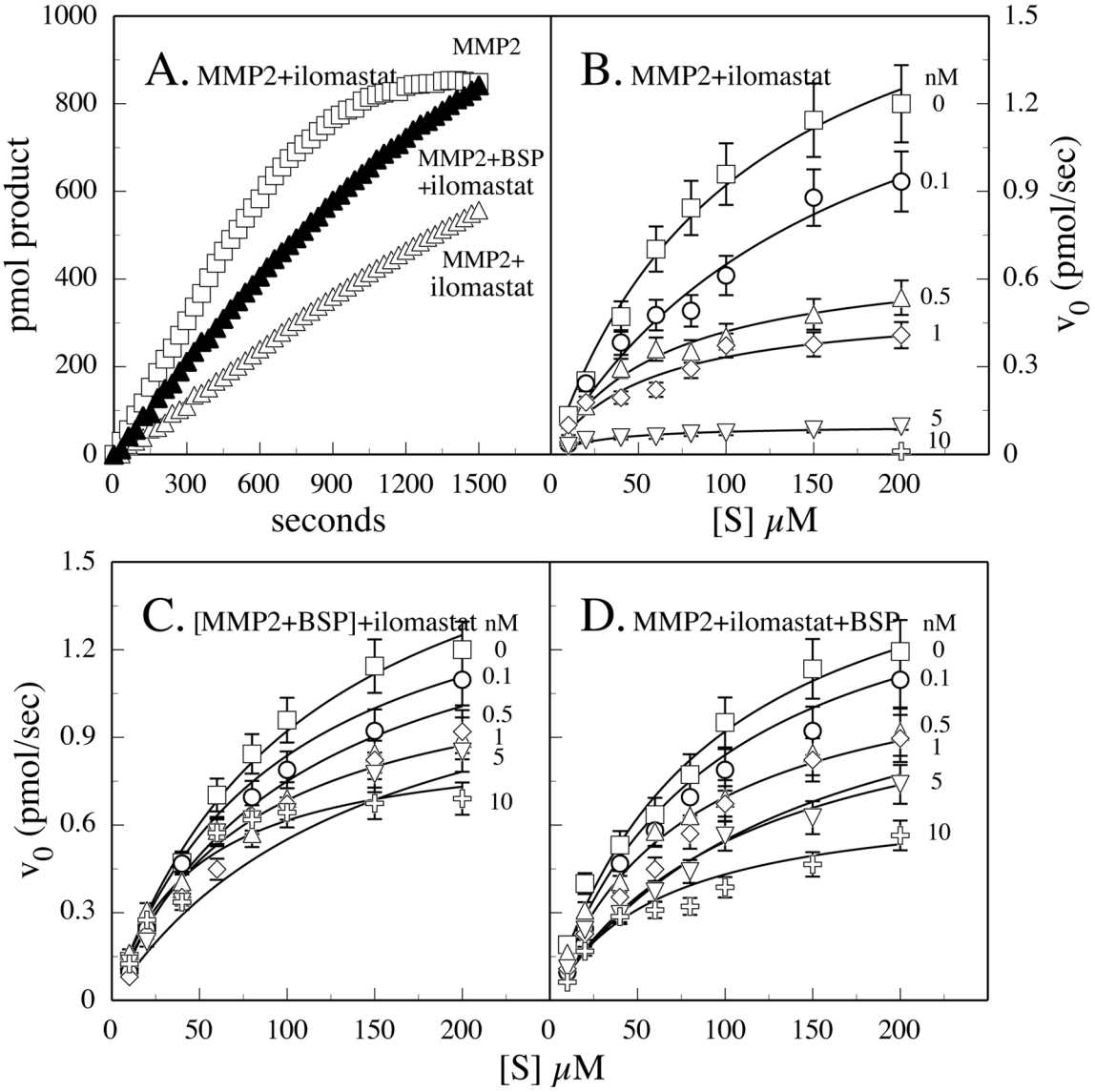

FIGURE 2.

Effects of BSP on ilomastat inhibition of MMP-2. Peptide substrate (100 μM) was incubated with 10 nM MMP-2 (□), 10 nM MMP-2 and 1 nM ilomastat (▵), or 10 nM MMP-2, 10 nM BSP, and 1 nM ilomastat (▲) and the evolution of product followed by absorbance at 405 nm (A). We generated substrate-velocity plots by increasing the substrate concentration at different fixed inhibitor concentrations with the slope over the first 6 min being used to calculate V_0 values (B–D). Active MMP-2 was incubated with ilomastat whose concentration varied: 0 (□), 0.1 (○), 0.5 (▵), 1 (◇), 5 (▽), and 10 nM (+). Inhibitor and substrate titrations were carried out by adding the inhibitor to (B) MMP-2, (C) an MMP-2-BSP preformed complex, or (D) simultaneously added 10 nM MMP-2 and BSP.

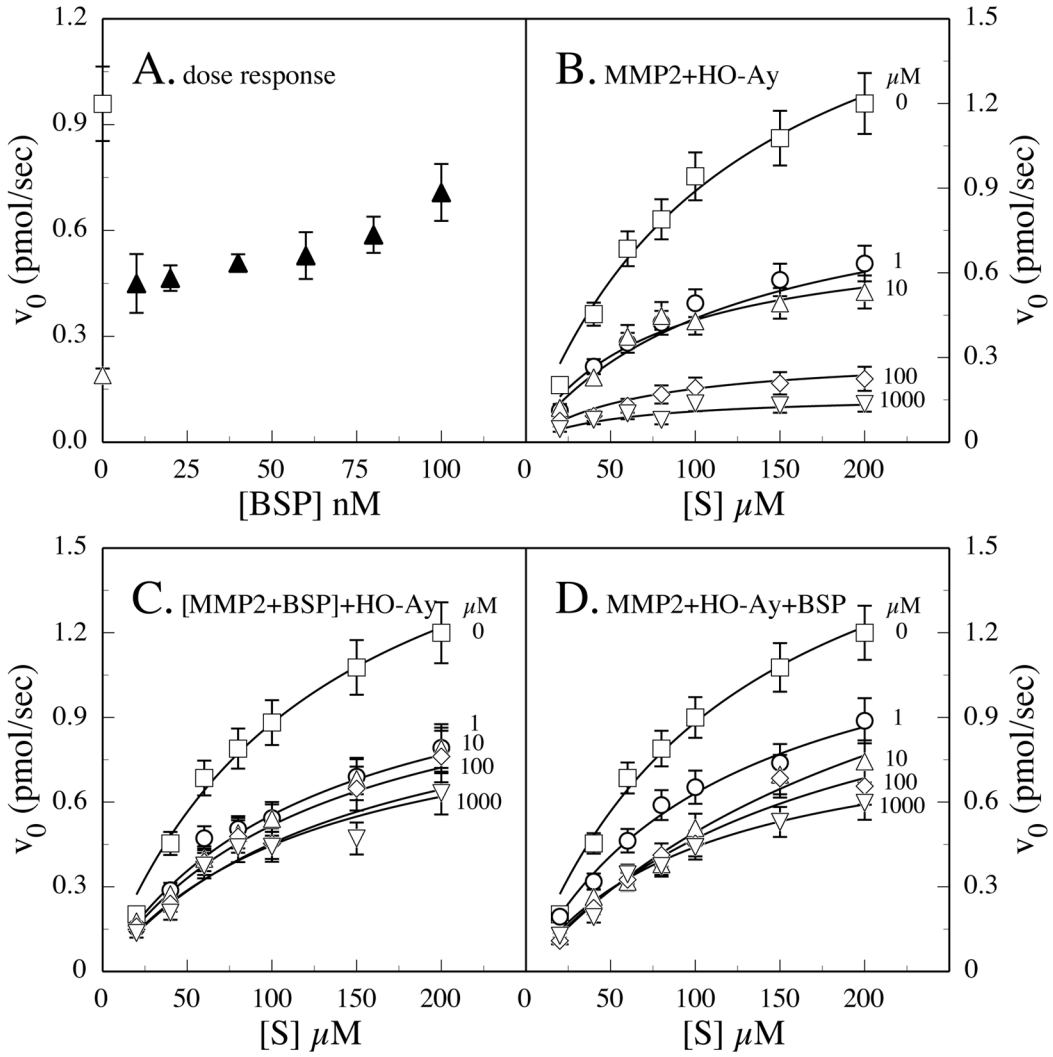

FIGURE 3.

Effects of BSP on oleoyl-*N*-hydroxylamide (HO-Ay) inhibition of MMP-2. Peptide substrate (100 μM) was incubated with 10 nM MMP-2 (□), 10 nM MMP-2 and 1 nM HO-Ay (▵), or 10 nM MMP-2, 1 nM HO-Ay, and varying concentrations of BSP (▲), and the evolution of product followed by absorbance at 405 nm over the first 6 min of the reaction was used to profile a dose response of BSP restoration of activity (A). Substrate-velocity plots were generated by increasing substrate concentrations at different fixed inhibitor concentrations with the slope over the first 6 min being used to calculate V_0 values (B–D). Active MMP-2 was incubated with HO-Ay, whose concentration varied: 0 (□), 1 (○), 10 (▵), 100 (◊), and 1000 μM (▽). Inhibitor and substrate titrations were made by adding the inhibitor to (B) MMP-2, (C) an MMP-2-BSP preformed complex, or (D) simultaneously added 10 nM MMP-2 and BSP.

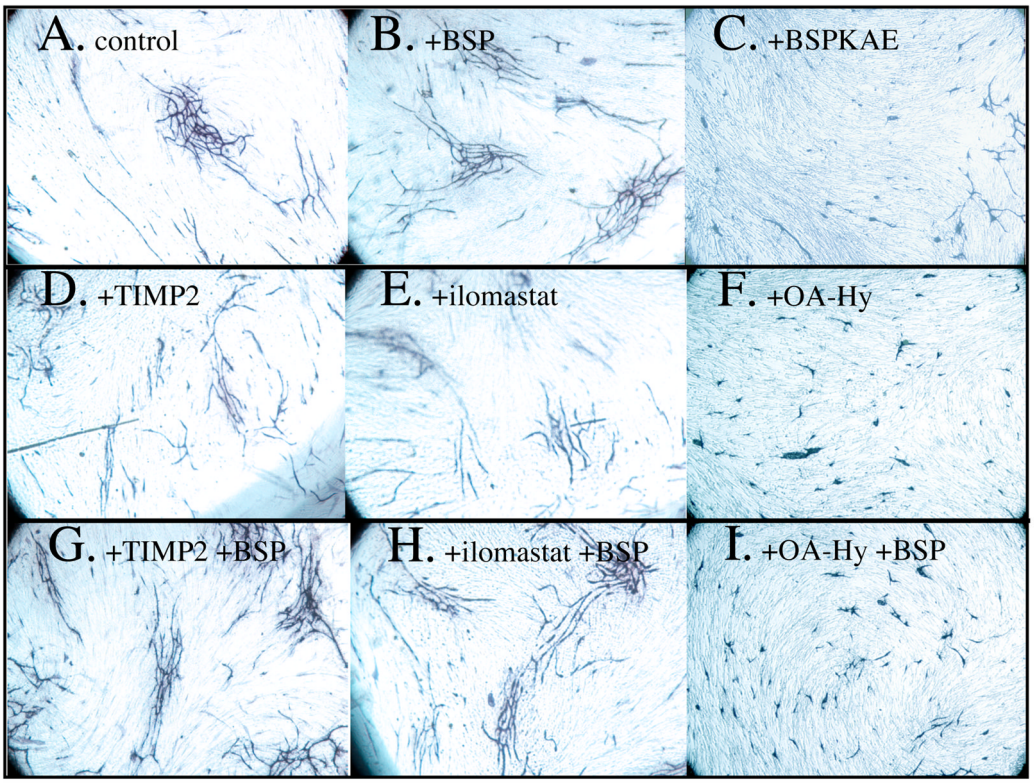

FIGURE 4.

BSP stimulates angiogenesis and overcomes MMP-2 inhibitors in vitro. HUVECs cocultured with fibroblasts were treated starting on day 6 of culture with (A) vehicle alone, (B) 5 nM BSP, (C) 5 nM BSPKAE, (D) 5 nM TIMP2, (E) 5 nM ilomastat, (F) 33.6 nM oleoyl-*N*-hydroxylamide (HO-Ay), (G) 5 nM BSP and 5 nM TIMP2, (H) 5 nM BSP and 5 nM ilomastat, or (I) 5 nM BSP and 33.6 nM oleoyl-*N*-hydroxylamide. The cells were fixed on day 12 and probed with a PECAM1 antibody (blue) to visualize tubule formation. Note that BSP stimulated tubule formation and in equimolar amounts reversed the inhibitory

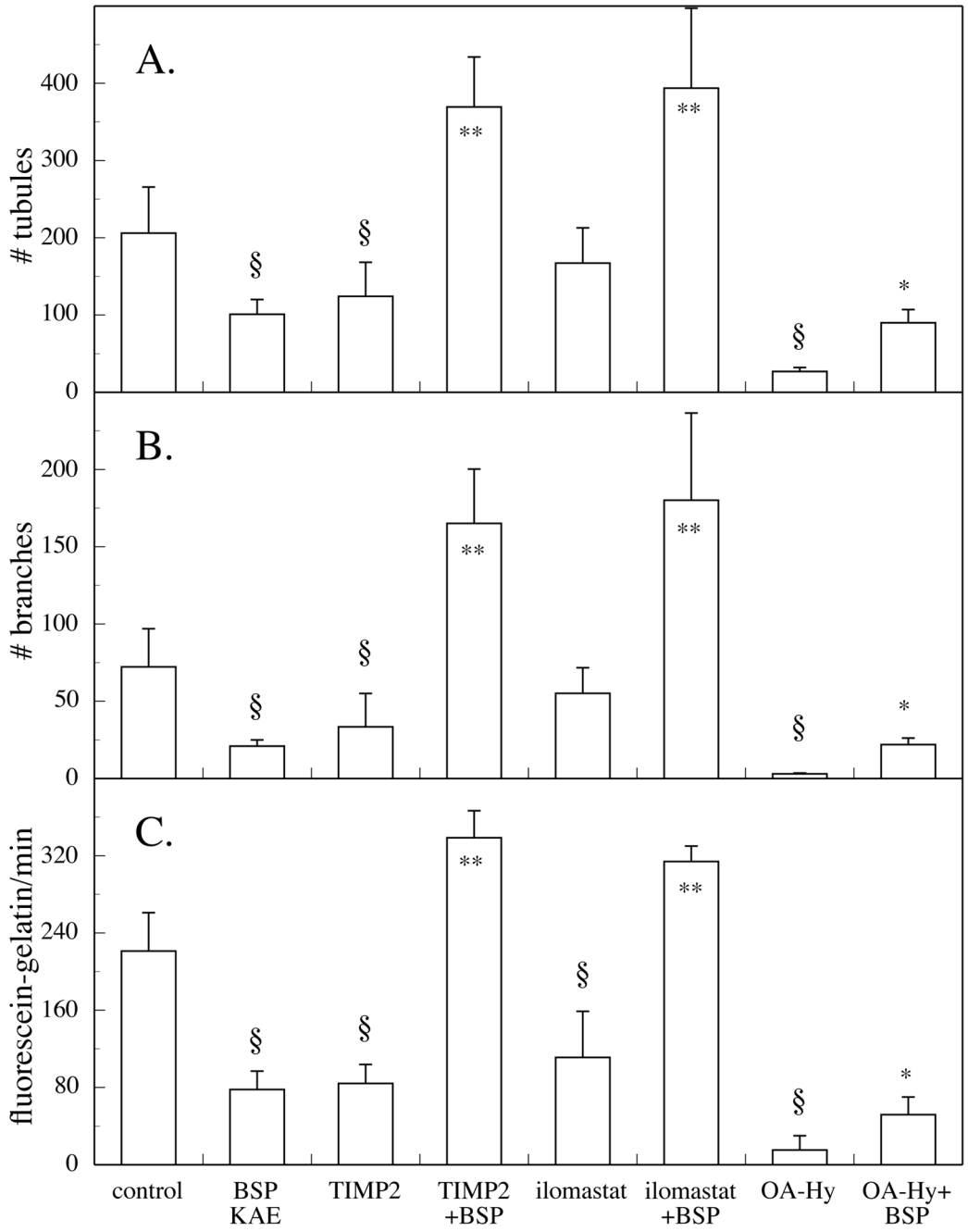

FIGURE 5.

Quantification of the effects of recombinant BSP on tubule formation and in overcoming the effects of MMP-2 inhibitors. Two distinct fields from each triplicate well of the experimental conditions described were digitized as .tif files and analyzed using AngioSys version 1.0 (TCS Cell Works). The image analysis package determined the number of tubules (A) and the number of branch points or junctions (B) between tubules. In addition, a cell surface-associated pool from day 10 cohort cultures was assayed for MMP activity by the large fluorescein-gelatin substrate assay (C). The § symbol represents an ANOVA p value of ≤ 0.05 for comparing control values vs with inhibitor. Asterisks represent t test p values with of ≤ 0.05 (one asterisk) and ≤ 0.01 (two asterisks) for comparing each inhibitor with or without BSP.

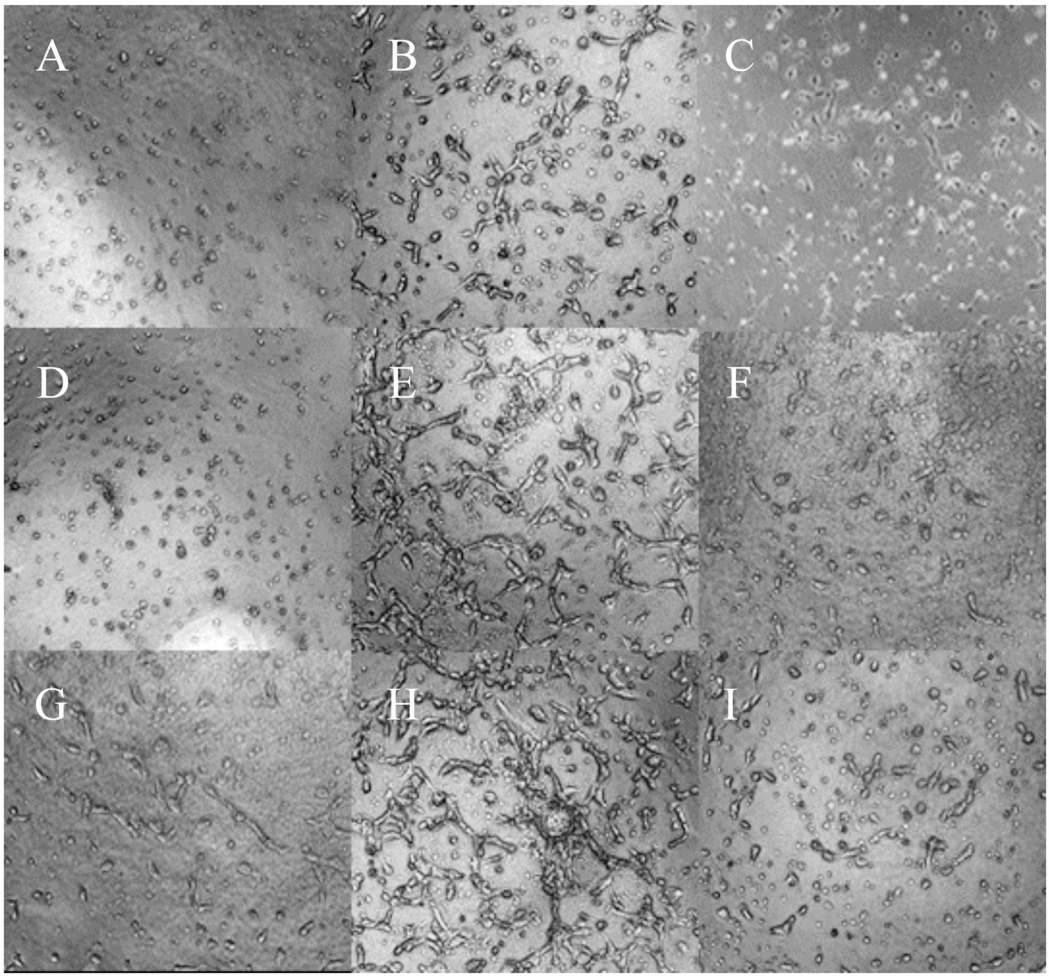

FIGURE 6.

BSP stimulation of HUVEC tubule formation is MMP-2-dependent. HUVECs that were transfected with an adenovirus encoding BSP or with null adenovirus were transferred onto type I collagen gels, and a second layer of collagen was layered on top of the adherent cells forming a collagen sandwich. A set of BSP adenovirus-transfected cells were also treated with an activity blocking antibody to MMP- 2. Null virus-transfected cells (A, D, and G), BSP virus-transfected cells (B, E, and H), and BSP adenovirus-transfected cells treated with 1.25 μg/mL MMP-2 antibody (C, F, and I) were visualized at 14 (A–C), 24 (D–F), and 48 h (G–I) on a Nikon Diaphot inverted microscope and digitized with a Polaroid CCD digital camera.

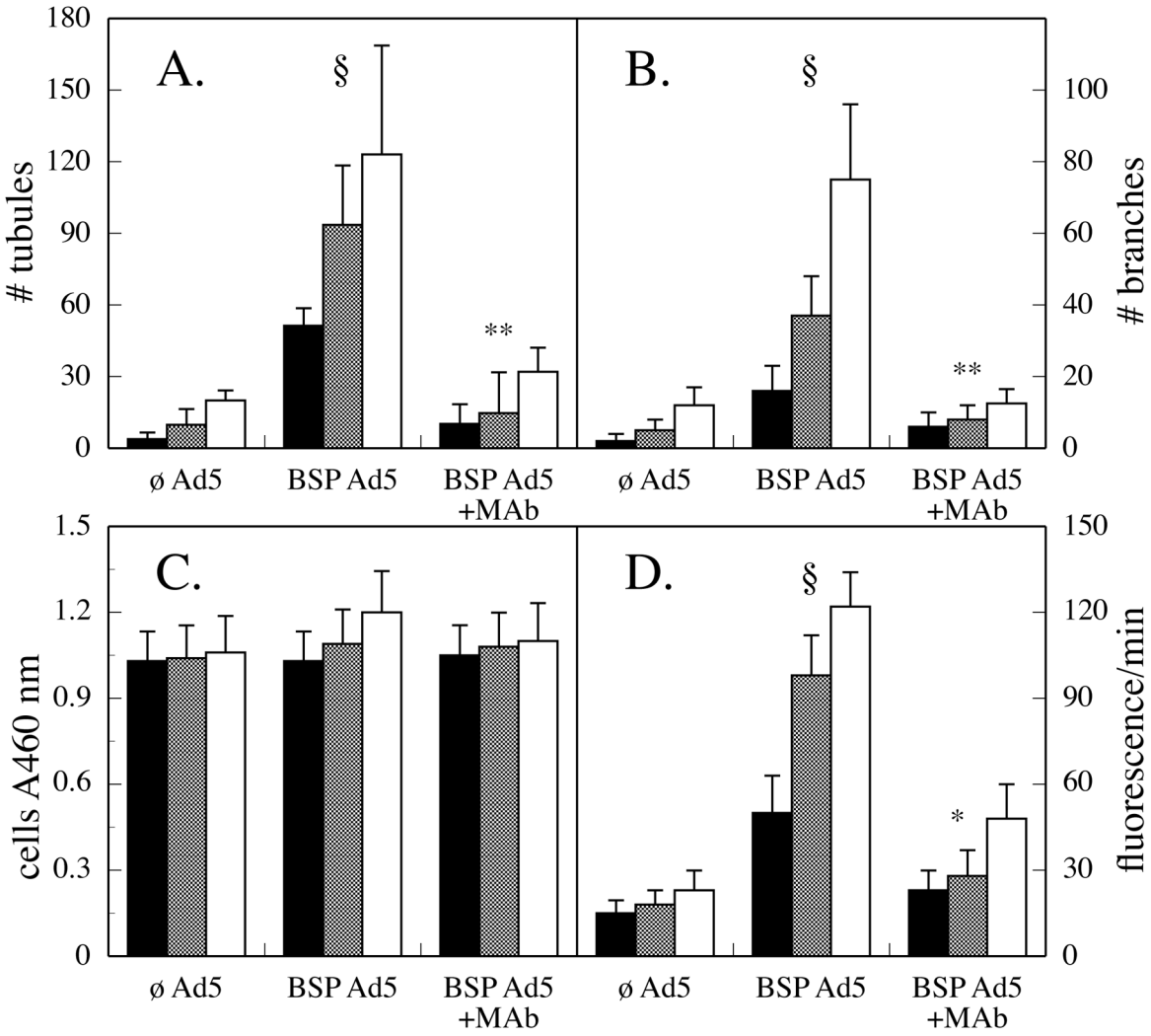

FIGURE 7.

Quantification of the effects of BSP expression on tubule formation. As in Figure 5, two distinct fields from each triplicate well of the null virus-transfected cells (øAd5), BSP adenovirus-transfected cells (BSP Ad5), and BSP adenovirus-transfected cells treated with MMP-2 antibody (BSP Ad5 + mAb) were digitized as .tif files and analyzed using AngioSys version 1.0. The number of tubules (A) and the number of branch points or junctions between tubules (B) were calculated. In addition, cell number was followed by absorbance using a water soluble MTT dye, CCK-8 (C), and MMP activity (D) was assayed by following fluorescein emission in wells where the large fluorescein-gelatin substrate had been incorporated into the collagen gel (C). The time points analyzed were 14 h (black bars), 24 h (gray bars), and 48 h (white bars). The § symbol represents a paired *t* test *p* value of ≤0.001 for comparing null virus- to BSP virus-transfected cells across the different time points. Asterisks represent *t* test *p* values of ≤0.01 (one asterisk) and ≤0.001 (two asterisks) for comparing BSP virus-transfected cells with or without MMP-2 antibody across the different time points.

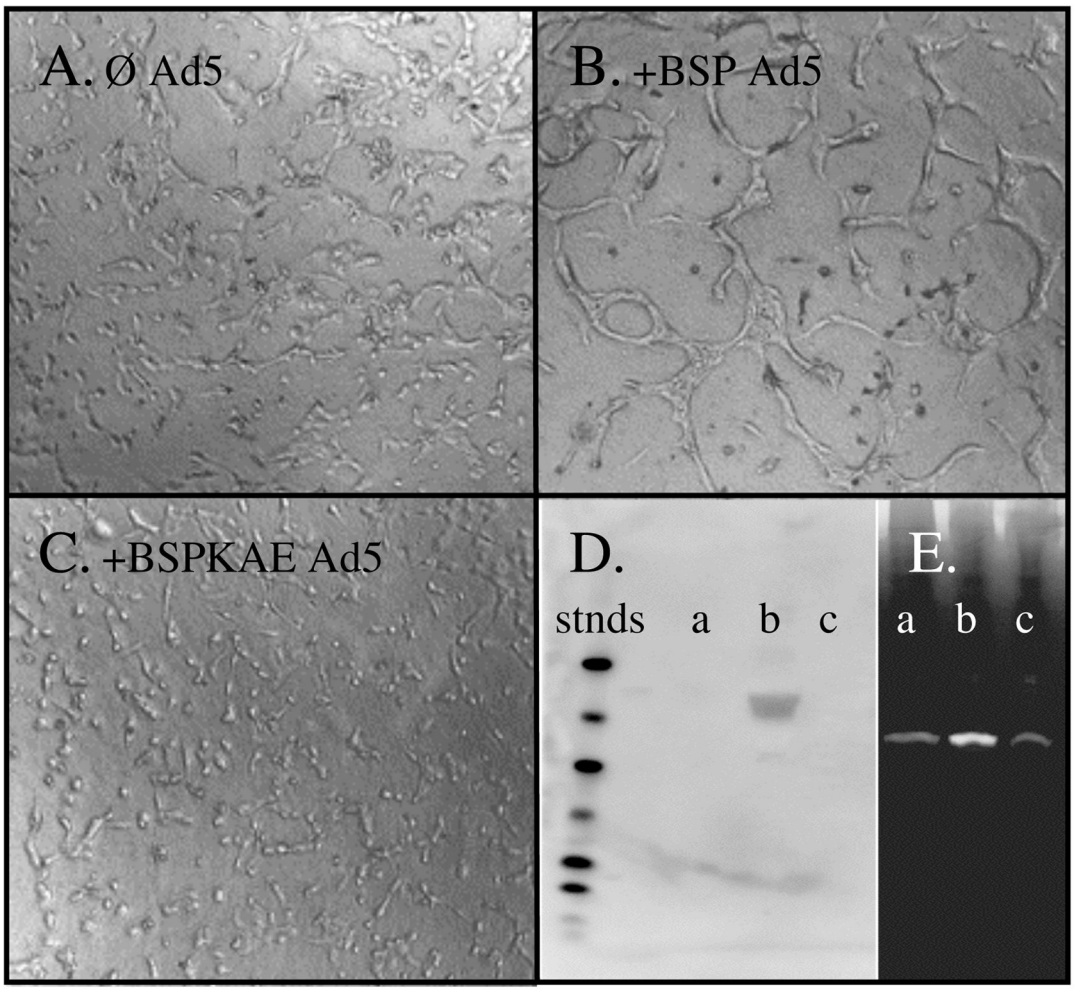

FIGURE 8.

BSP increases the level of active MMP-2 cell surface localization during tubulogenesis. HUVECs that were transfected with an adenovirus encoding BSP or BSPKAE or with null adenovirus were transferred into type I collagen gels. Null virus-transfected (A), BSP-transfected (B), and BSPKAE-transfected (C) cells were visualized at 24 h with a Nikon Diaphot inverted microscope and digitized with a Polaroid CCD digital camera. Plasma membrane-associated pools were generated from the different conditions and analyzed for BSP protein levels by Western blot (D) and for active MMP-2 levels by zymography (E).

Table 1

Bone sialoprotein effects on matrix metalloproteinase-2 kinetic parameters.

	K_m [a]	V_{max}	K_{ic} [b]	K_{iu} [b]
MMP2 [c]	103 ± 14	1.9 ± 0.1		
MMP2 + BSP	90 ± 10	2.1 ± 0.2		
MMP2+ TIMP2	103 ± 9	1.9 ± 0.8	0.67 ± 0.06	1.4 ± 0.2
[MMP2+BSP] + TIMP2	127 ± 18	2.1 ± 0.2	24 ± 12	9 ± 4
MMP2 + TIMP2 + BSP	98 ± 14	1.8 ± 0.1	10 ± 2	8 ± 2
MMP2+ ilomastat	106 ± 23	1.8 ± 0.5	0.3 ± 0.1	-
[MMP2+BSP]+ ilomastat	85 ± 14	1.5 ± 0.1	14 ± 4	-
MMP2 + ilomastat + BSP	88 ± 10	1.6 ± 0.2	9.8 ± 0.3	-
MMP2 + OA-Hy	97 ± 14	1.9 ± 0.3	5.9 ± 0.4	-
[MMP2+BSP]+ OA-Hy	127 ± 22	2.1 ± 0.4	150 ± 47	-
MMP2 + OA-Hy +BSP	135 ± 25	2.2 ± 0.5	106 ± 48	-

[a] For the substrate Ac-PLG-[2-mercapto-4-methyl-pentanoyl]-LG-OC_2H_5, K_m values are μM.

[b] K_{ic} and K_{iu} values were determined by fitting the generalized linear mixed inhibition equation. K_{ic} values for TIMP2 and ilomastat are nM, while OA-Hy is μM.

[c] Abbreviations: MMP2, matrix metalloproteinase-2; BSP, bone sialoprotein; TIMP2, tissue inhibitor of matrix metalloproteinase-2; OA-Hy, oleoyl-N-hydroxylamide.